Supporting Information

Morphology, local stoichiometry and photoexcited states in Cu@Cu_2O nanostructured systems grown by physical synthesis

Eleonora Spurio[1], Francesca Alimonti[1], Giovanni Bertoni[1], Sergio D'Addato[1,2], Giuseppe Ammirati[3], Alessandra Paladini[4], Stefano Turchini[3], Daniele Catone[3], Patrick O'Keeffe[4], Paola Luches[1*]

[1] CNR-Istituto Nanoscienze (CNR-NANO), Via G. Campi 213/a, 41125 Modena, Italy

[2] Dipartimento di Fisica Informatica e Matematica, Università di Modena e Reggio Emilia, 41121 Modena, Italy

[3] CNR-Istituto di Struttura della Materia (CNR–ISM), EuroFEL Support Laboratory (EFSL), Via del Fosso del Cavaliere 100, 00133 Rome, Italy

[4] CNR-Istituto di Struttura della Materia (CNR-ISM), EuroFEL Support Laboratory (EFSL), Monterotondo Scalo 00015, Italy

Corresponding author e-mail: paola.luches@nano.cnr.it

Statistical analysis of STEM images

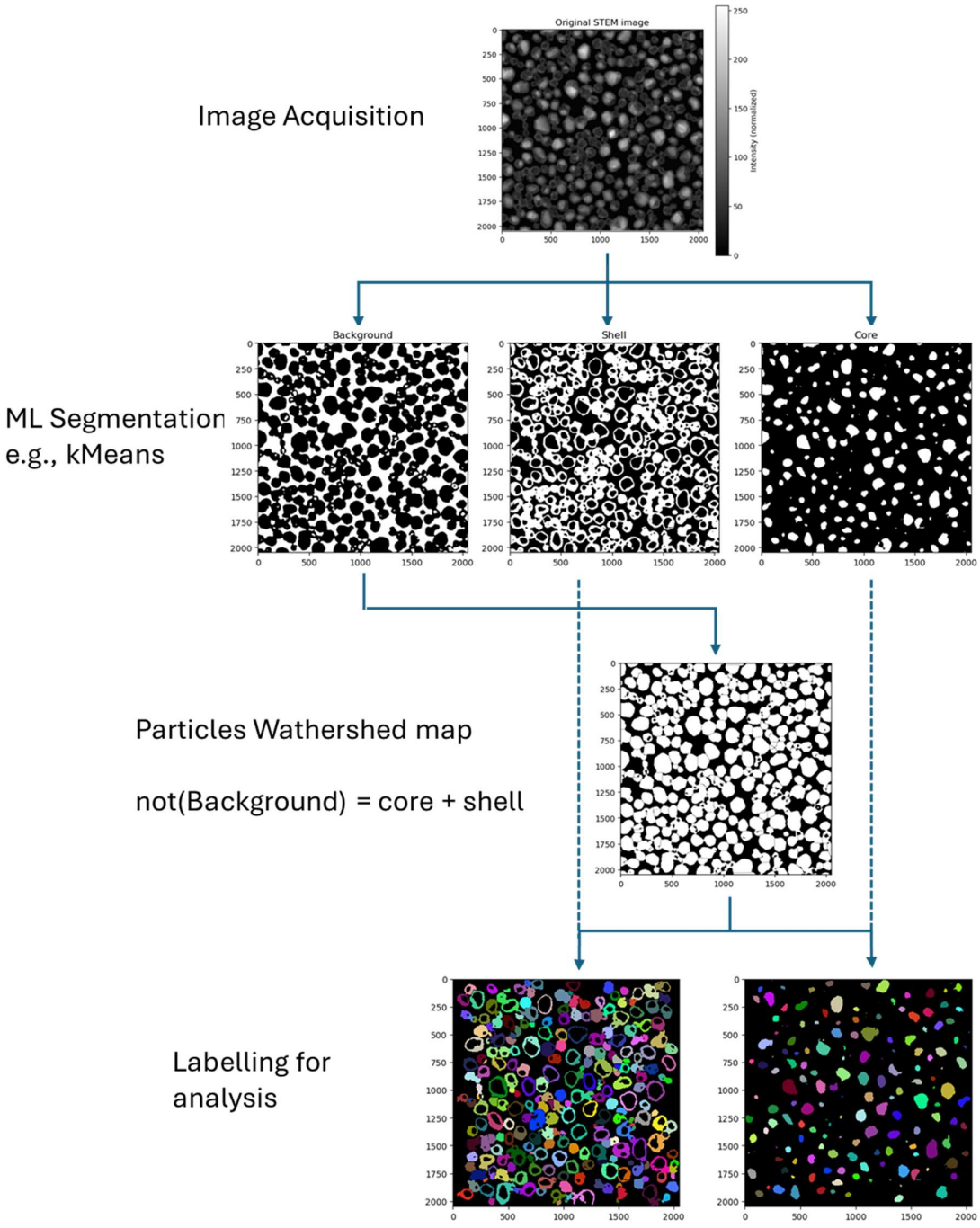

Figure S1: Schematics of the automated core/shell particles analysis. After image acquisition, an unsupervised machine learning-based segmentation algorithm is applied in place of standard thresholding, and the three classes (maps) are identified and ordered in term of increasing contrast as background, shell, and core. To separate touching shells, a watershed separation is applied to the inverted background map and used to multiply the core and shell

maps. These are finally labelled and analyzed to extract the quantitative parameters and histograms (in-plane core diameters and thickness of the shells).

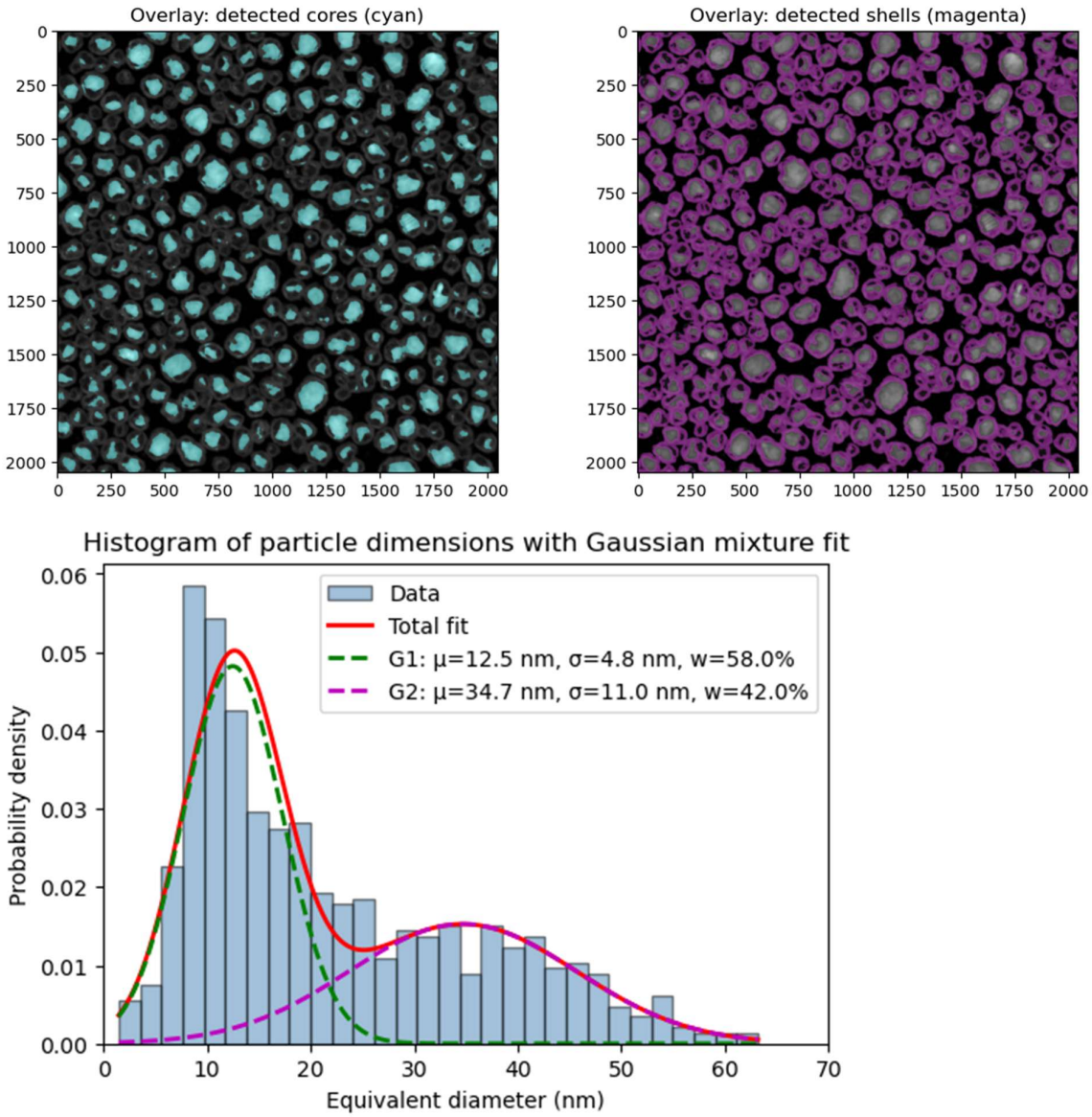

Particle size (nm): mean = 21.79 nm, std = 13.56 nm

Core size (nm): mean = 14.92 nm, std = 10.34 nm

Shell thickness (nm): mean = 3.98, std = 0.70

Figure S2: Top: STEM image of the sample obtained from a 6 nm Cu film after a treatment in a furnace in O_2/N_2 flux at 373 K for 30 min (Figure 1a of the main text) with core-related mask (left) and shell-related mask (right). Bottom: histogram of in-plane particle size with multi-gaussian fitting. The average particle size, core size and shell thickness are also reported.

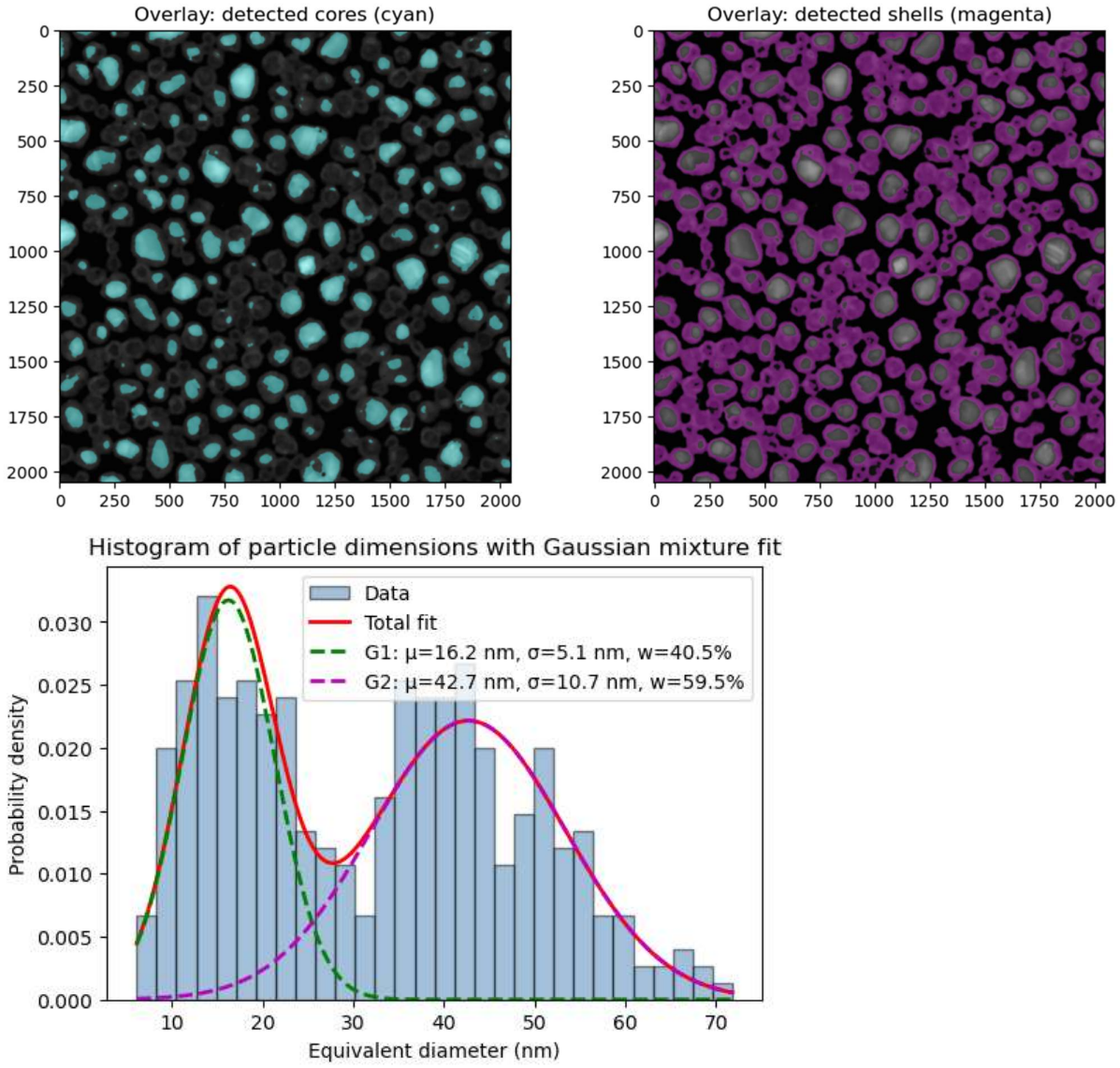

Particle size (nm): mean = 31.99 nm, std = 15.73 nm

Core size (nm): mean = 21.57 nm, std = 12.63 nm

Shell thickness (nm): mean = 6.05, std = 1.82

Figure S3: Top: STEM image of the sample shown in Figure S2 after annealing at 773 K in UHV for 30 min (Figure 1b of the main text) with core-related mask (left) and shell-related mask (right). Bottom: histogram of in-plane particle size with multi-gaussian fitting. The average particle size, core size and shell thickness are also reported. The main effect of the reducing

treatment on the morphology is to modify the relative weight of the two peaks in the size distribution.

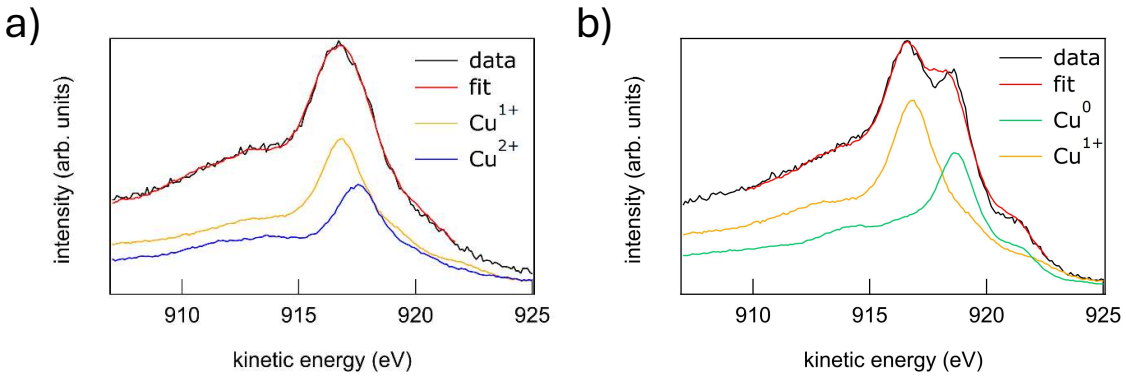

Figure S4: Cu $L_{23}M_{45}M_{45}$ AES spectra, fit and fitting components, related to the 6 nm Cu film after a treatment in a furnace in O_2/N_2 flux at 373 K for 30 min (panel a - c_{Cu1+}=40%, C_{Cu2+}=60%) and annealing at 773 K in UHV for 30 min (panel b - c_{Cu0}=45%, C_{Cu1+}=55%) (Figure 2b of the main text).

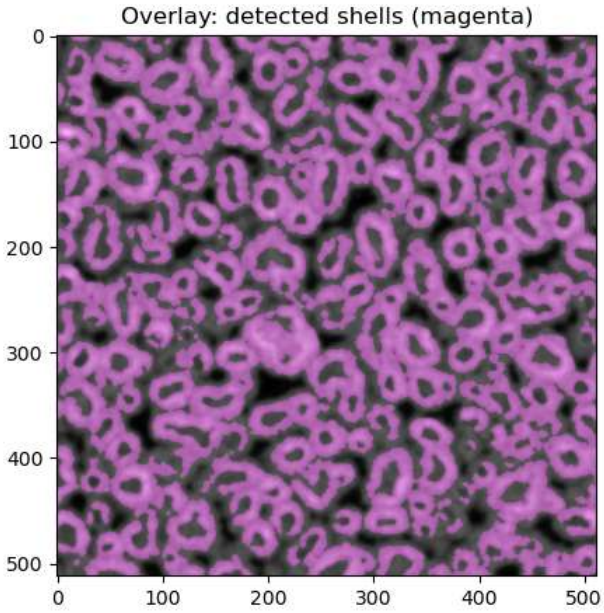

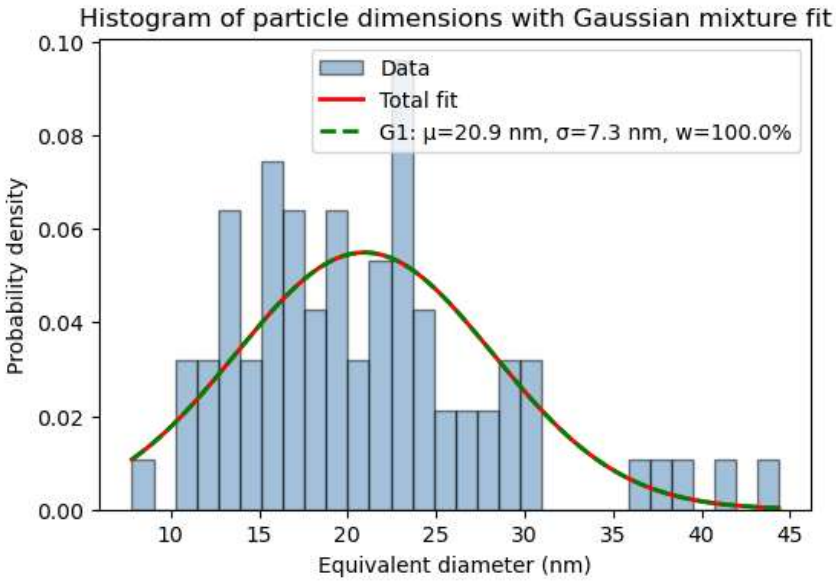

Particles size (nm): mean = 20.95, std = 7.26

Shell thickness (nm): mean = 2.48, std = 0.49

Figure S5: Top: STEM image of the Cu_2O sample obtained from a 2 nm Cu film after oxidation at 423 K in O_2/N_2 flux for 40 min and reduction at 623 K in UHV for 30 min (Figure 3a of the main

text) with shell-related mask. Bottom: histogram of in-plane particle size with gaussian fitting. The average particle size, and shell thickness are also reported.

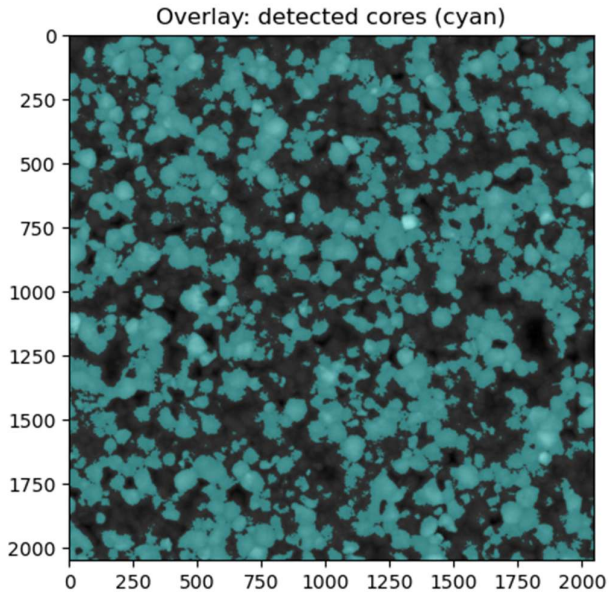

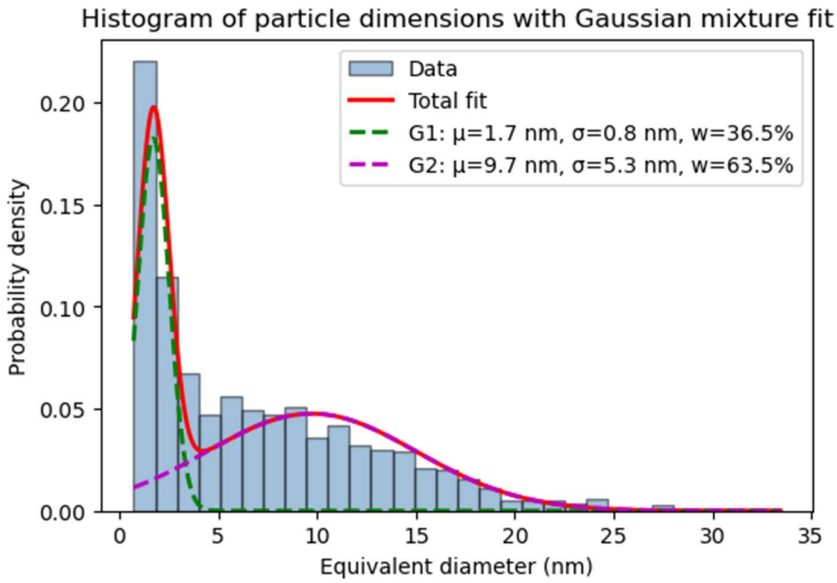

Particles size (nm): mean = 6.81, std = 5.75

Figure S6: Top: STEM image of the Cu_2O sample obtained from a 6 nm Cu film after oxidation at 423 K in O_2/N_2 flux for 60 min and reduction at 623 K in UHV for 30 min (Figure 3b of the main text) with core-related mask. Bottom: histogram of in-plane particle size with multi-gaussian fitting. The average particle size is also reported.

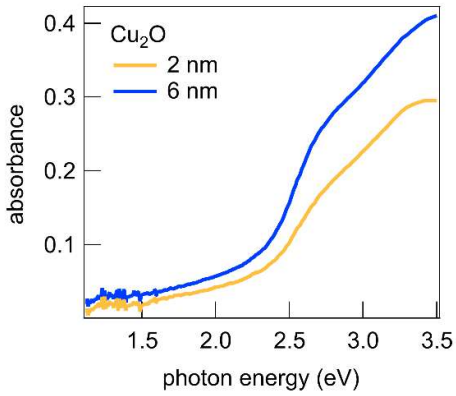

Figure S7: UV-Vis absorbance spectra of the 2 nm and 6 nm Cu_2O samples. The close similarity of the spectra, with a sharp absorption increase above 2.5 eV, and the absence of plasmon-related absorption features, demonstrate that both samples have a dominant Cu_2O stoichiometry.

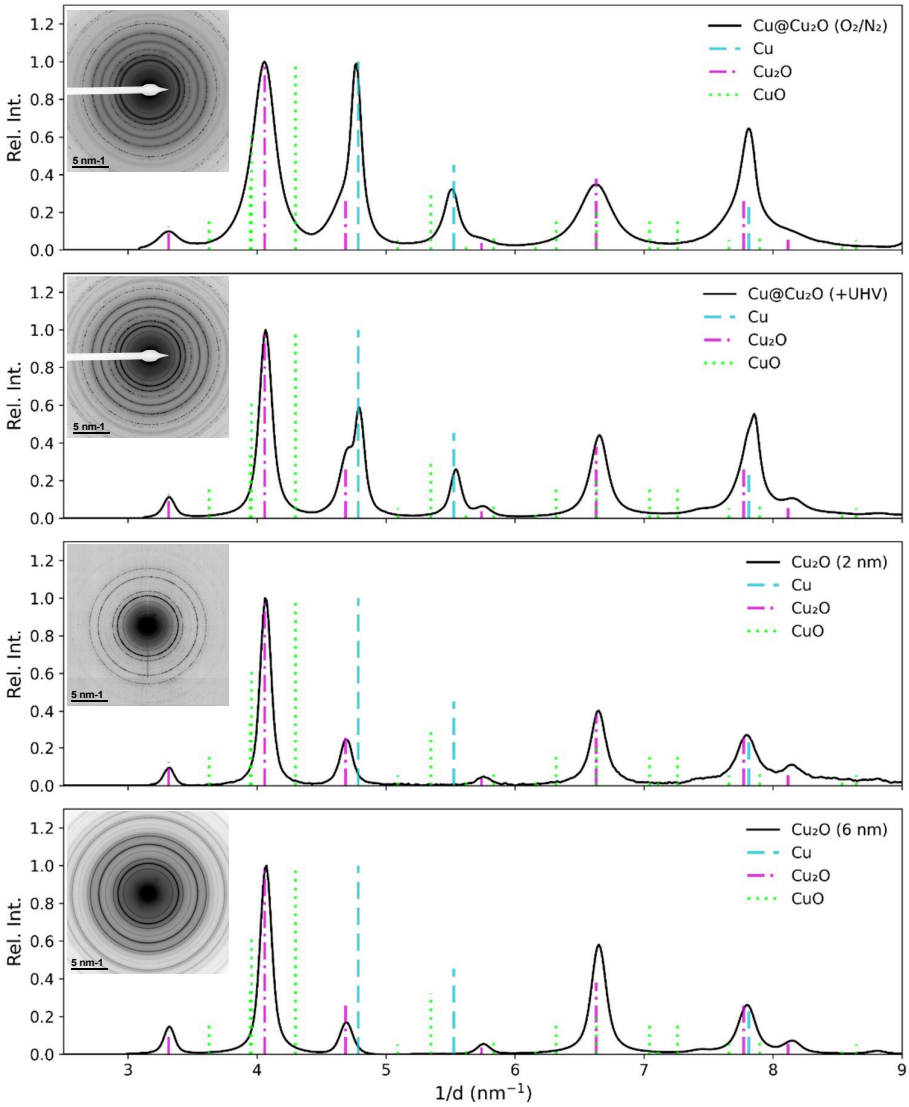

Figure S8: Azimuthally averaged TEM selected-area electron diffraction (SAED) profiles of the core–shell nanoparticles before and after reduction, and of the 2 nm and 6 nm Cu_2O samples. The profiles were obtained by azimuthal integration of the SAED patterns (shown as insets) followed by background subtraction. Vertical markers indicate the positions of crystallographically allowed reflections based on d-spacings, while their relative intensities are calculated in the kinematical electron diffraction approximation.

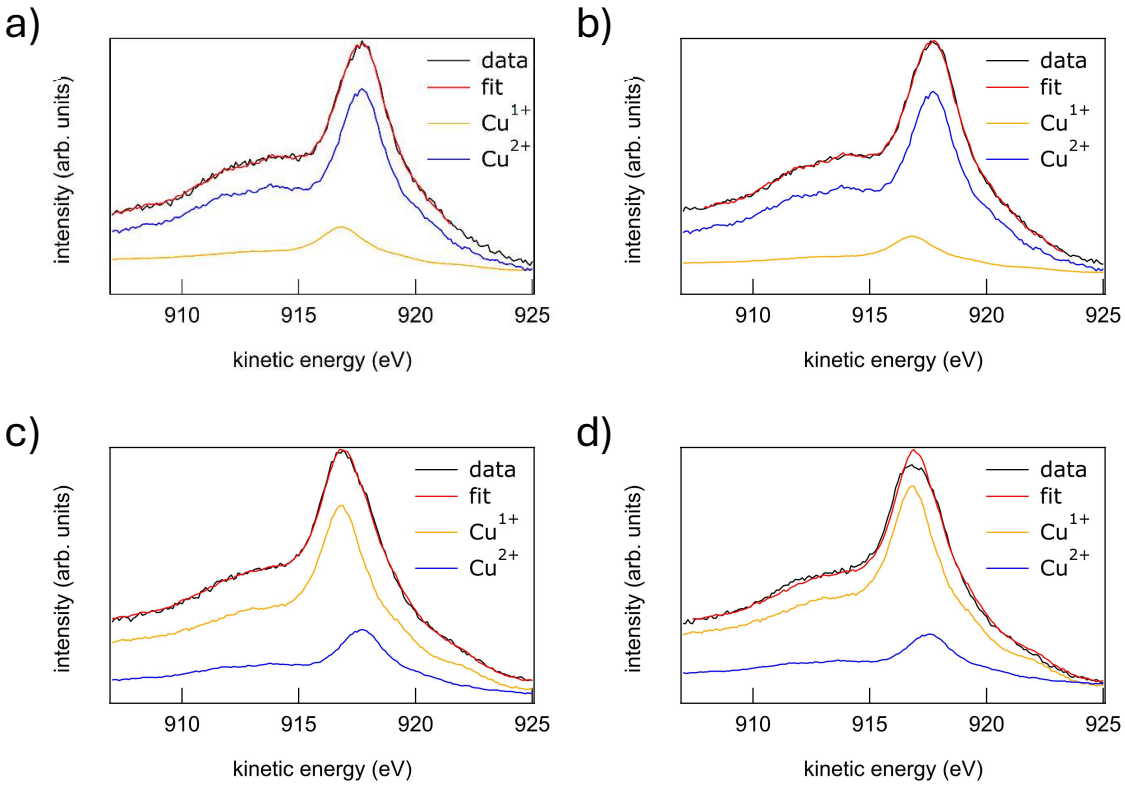

Figure S9: $L_{23}M_{45}M_{45}$AES spectra, fit and fitting components, of the 2 nm Cu film after film after oxidation at 423 K in O_2/N_2 flux for 40 min (panel a - c_{Cu1+}=14%, C_{Cu2+}=86%) and reduction at 623 K in UHV for 30 min (panel c - c_{Cu1+}=66%, C_{Cu2+}=34%) (Figure 4c of the main text); 6 nm Cu film after oxidation at 423 K in O_2/N_2 flux for 60 min (panel b - c_{Cu1+}=12%, C_{Cu2+}=88%) and reduction at 623 K in UHV for 30 min (panel c - c_{Cu1+}=73%, C_{Cu2+}=27%) (Figure 4d of the main text).

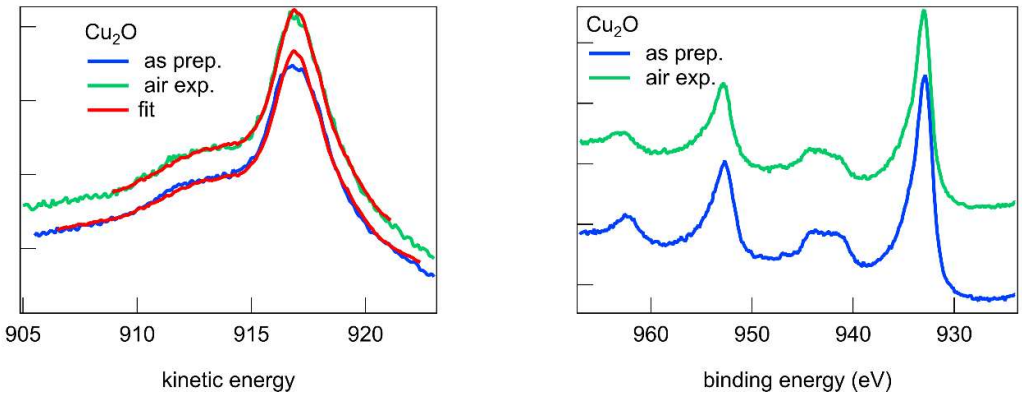

Figure S10: Cu $L_{23}M_{45}M_{45}$ AES and Cu 2p XPS spectra of the 6 nm Cu_2O sample before and after air exposure. The fit of the AES spectra results in Cu^{2+} concentrations that are (27 ± 3) % before air exposure and (31 ± 3) % after air exposure.